nature protocols

https://doi.org/10.1038/s41596-023-00848-1

Protocol

Microlensed fiber allows subcellular imaging by laser-based mass spectrometry

In the format provided by the authors and unedited

Supplementary Materials for

Microlensed fiber allows subcellular imaging by laser-based mass spectrometry

Yifan Meng[1,2], Wei Hang[1]* and Richard N. Zare[2]*

1. Ministry of Education (MOE) Key Laboratory of Spectrochemical Analysis and Instrumentation, College of Chemistry and Chemical Engineering, Xiamen University, Xiamen, 361005, China
2. Department of Chemistry, Stanford University, Stanford, California 94305, United States

Corresponding author: Prof. Dr. Wei Hang Email: weihang@xmu.edu.cn

Prof. Richard N. Zare Email: zare@stanford.edu

First author: Dr. Yifan Meng Email: yfmeng@stanford.edu

Table of Contents

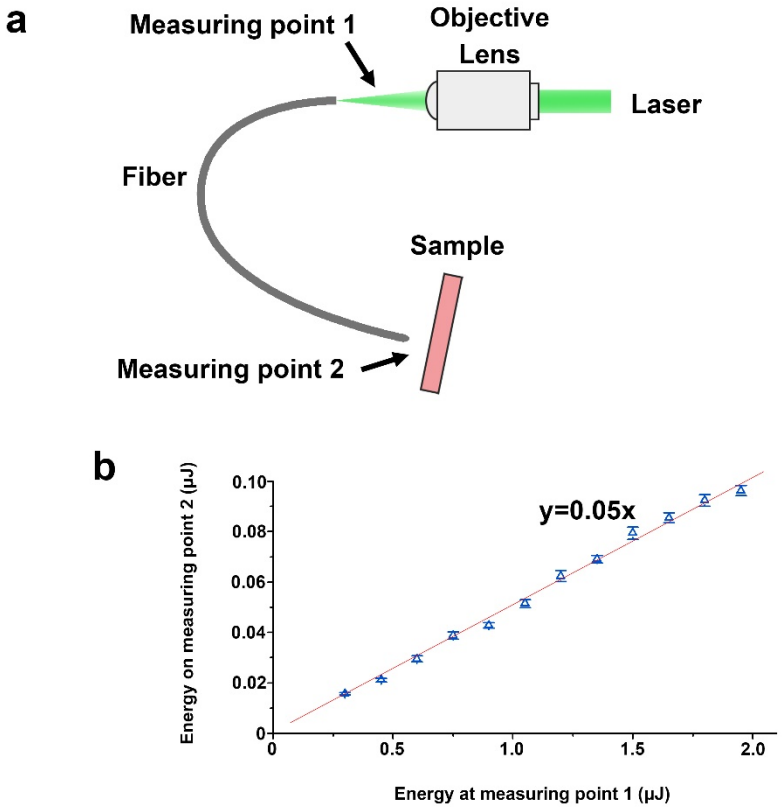

Supplementary Figure 1. Linear fitting of coupling efficiency. **a,** Schematic diagram of fiber coupling curve fitting method. It is not convenient to monitor the laser energy incident on the sample surface in vacuum chamber. By measuring the laser energy on point 1 (before entering into the fiber) and point 2 (output from the fiber), the desorption and ionization laser energy can be calculated accurately from the outside of the vacuum chamber. **b**, Relationship of laser energies at two measuring points. Normally, the laser energy applied to the sample is about tens of nanojoules.

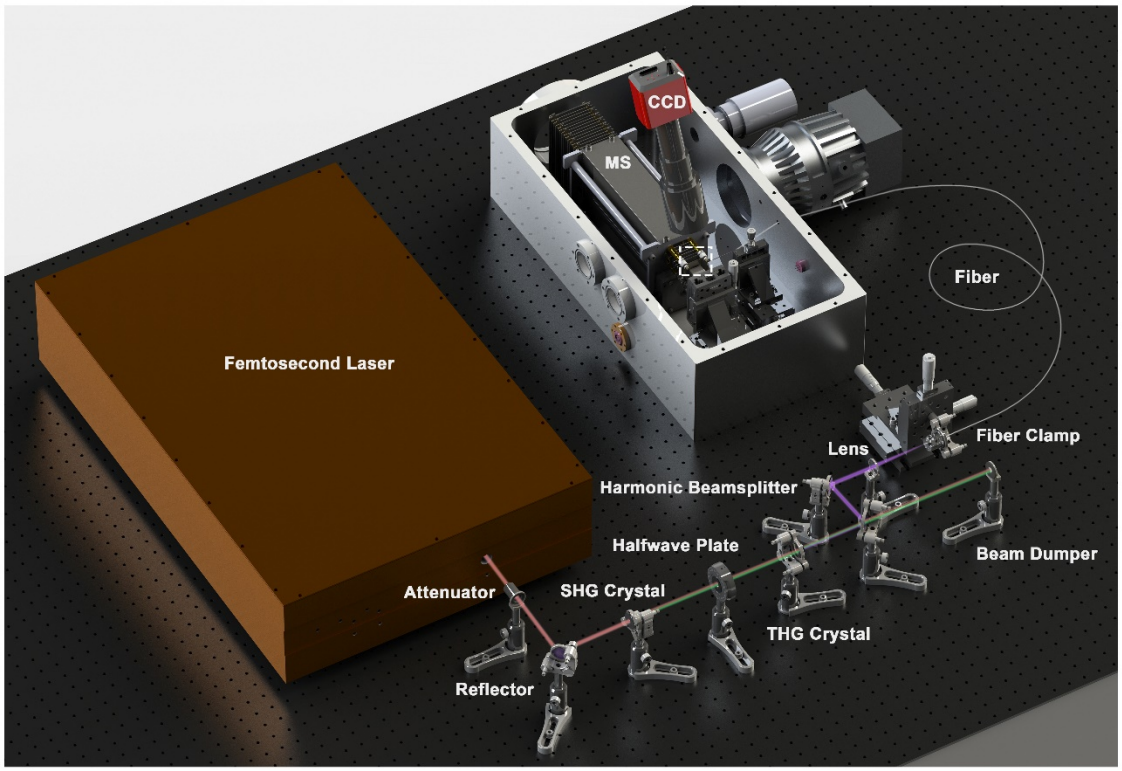

Supplementary Figure 2. Schematic diagram of the LDI-MSI platform.

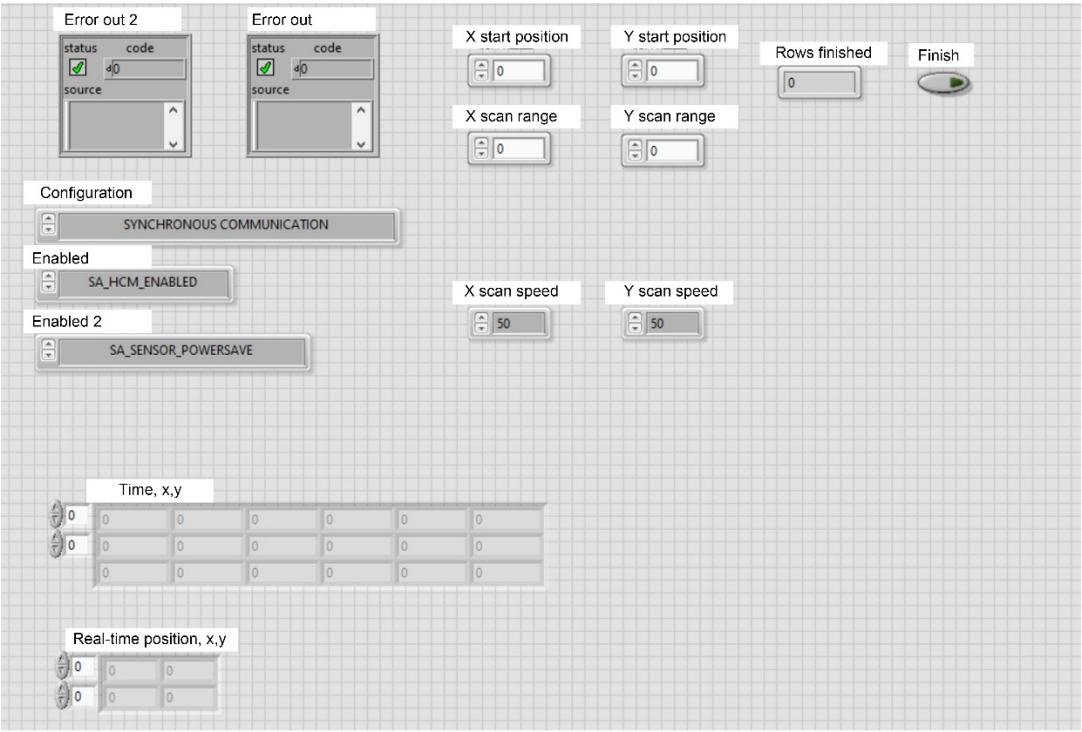

Supplementary Figure 3. The panel of the LabVIEW software for controlling the MSI process.

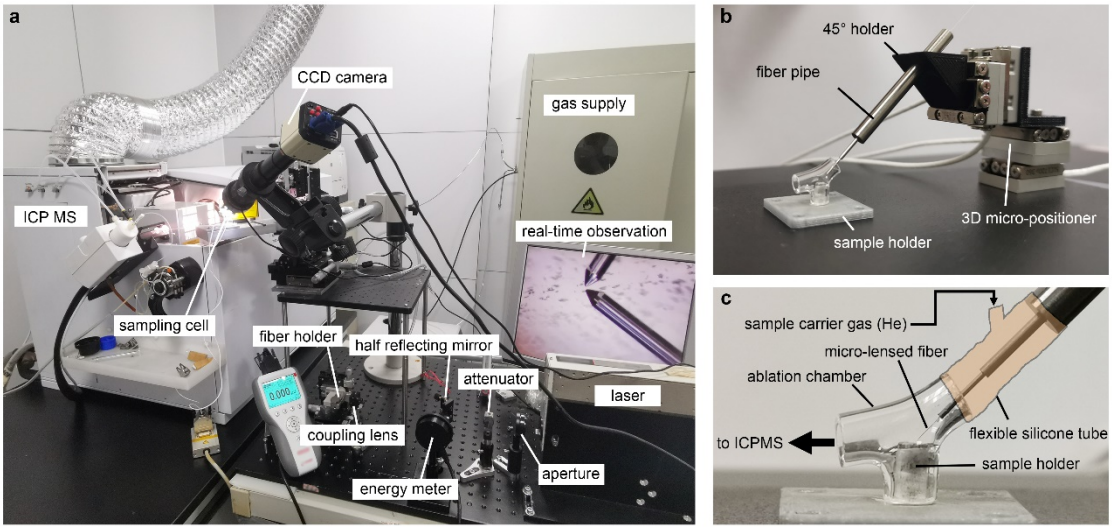

Supplementary Figure 4. Photograph of the LA-ICP-MSI platform based on the microlensed fiber. a, Overview of the operating platform. **b,** Nanoscale ablation chamber based on a microlensed fiber. **c,** Side-view of the ablation chamber.

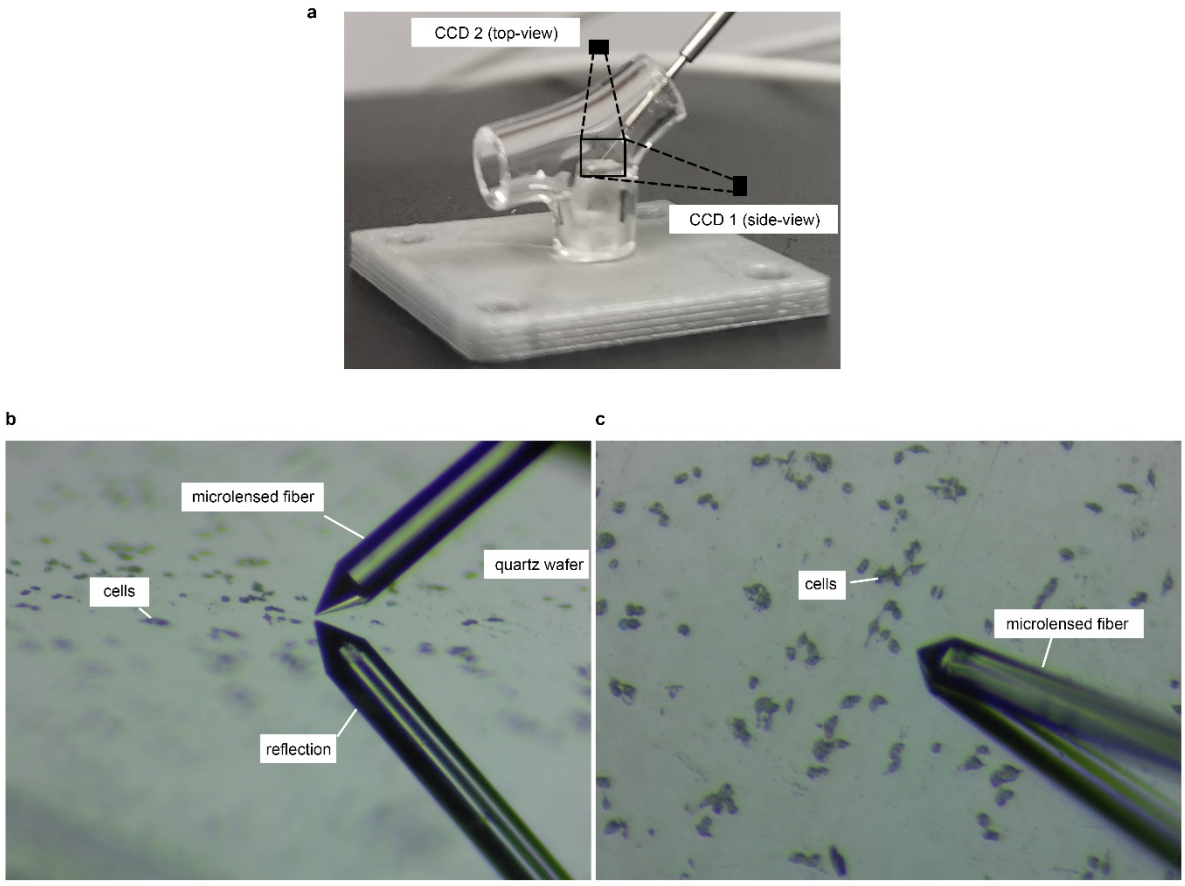

Supplementary Figure 5. Real-time observation system. **a,** Schematic diagram of the observation system with two CCD cameras. **b,** Real-time observation of HeLa cells from side-view. **c,** Real-time observation of HeLa cells from top-view.

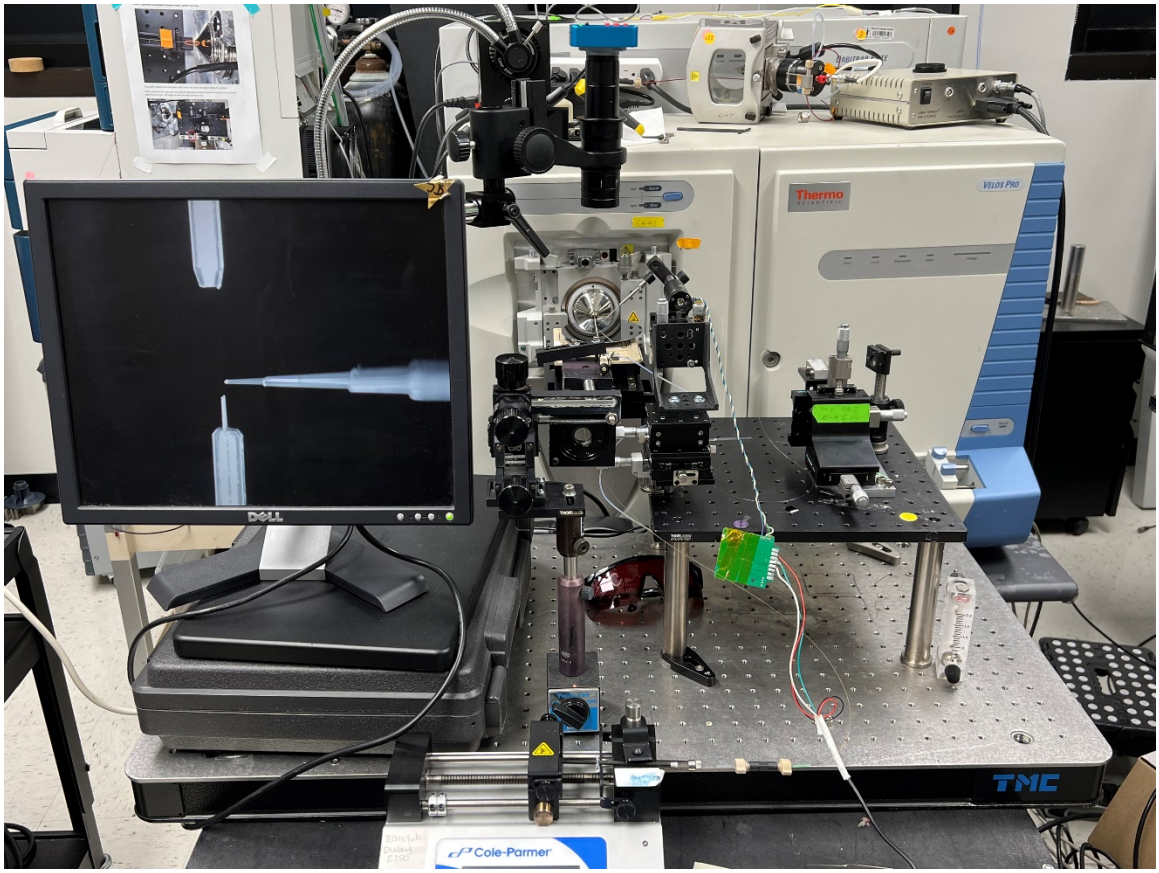

Supplementary Figure 6. A photo of the LA-ESI-MSI experimental setup.

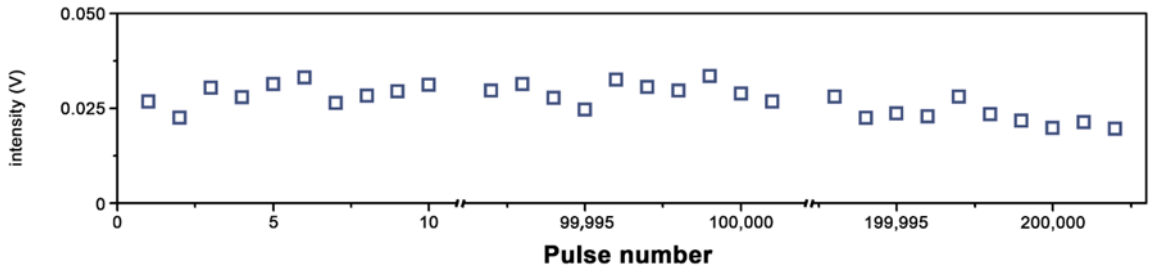

Supplementary Figure 7. Signal stability during 200,000 laser pulses on a proflavine tablet.

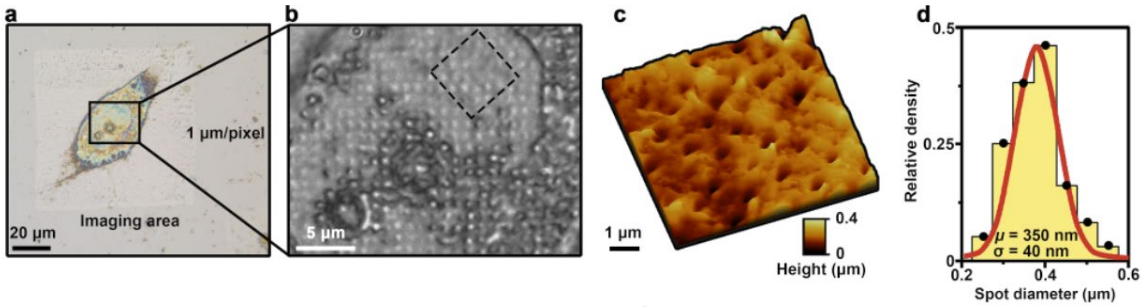

Supplementary Figure 8. **Sampling craters on a single cell.** (a) The optical image of a single cell while the region of interest is in light color. The step size is set as 1 μm. (b)The optical image of the outlined region in (a). White spots are sampling craters produced by the microlensed fiber. (c) An AFM image of the sampling craters on the cell outlined in (b). (d) The spot-size histogram showing a mean value of μ = 350 nm and an S.D. (standard deviation) of σ = 40 nm obtained by measuring 100 sampling spots.

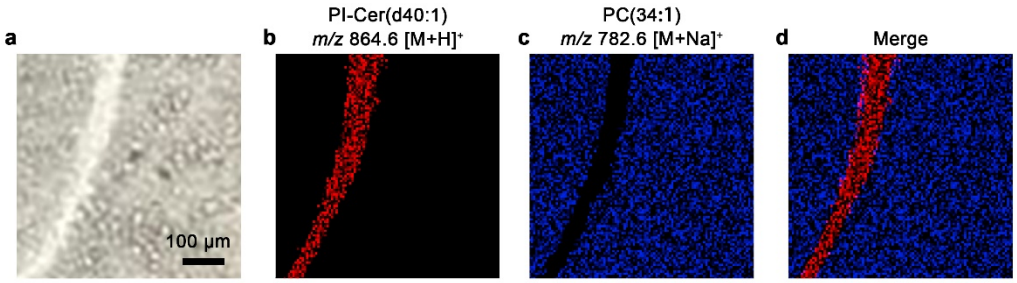

Supplementary Figure 9. Combining MALDI with microlensed fiber under atmospheric condition on a mouse brain tissue. (a) Optical image of the imaging area. (b) MS image of PI-Cer(d40:1) at *m/z* of 864.6. (c) MS image of PC(34:1) at *m/z* of 782.6. (d) Merged image of (b) and (c).

The experiment was carried out on a Q-TOF (Impact II, Bruker Corporation, MA, US) mass spectrometer. A nanosecond laser (355 nm, Minilite II, Continuum Electro-Optics, Inc., USA) was coupled into the multi-mode microlensed fiber and focused on a mouse brain tissue. Female BALB/c mice were anesthetized before being decapitated. The brain tissue was dissected from head and frozen at −80 °C, which was used for tissue section preparation. The mouse brain tissue sections of 12 μm thickness were obtained by using a cryostat (Leica CM1900, Germany), and the sections were thaw-mounted on indium–tin-oxide-coated glass slides. The sectioned mouse brain tissues were sprayed with DHB [20 mg/mL, acetonitrile/water (1:1, v/v) containing 0.1% trifluoroacetic acid] solution. The specific spraying conditions were as follows: 60 times of deposition, 3 s of spraying, 60 s of stewing, and 5 s of drying by purging with nitrogen. As shown in the following figure, we can obtain the image of two different lipids, PI-Cer(d40:1) at *m/z* of 864.6 and PC(34:1) at *m/z* of 782.6.

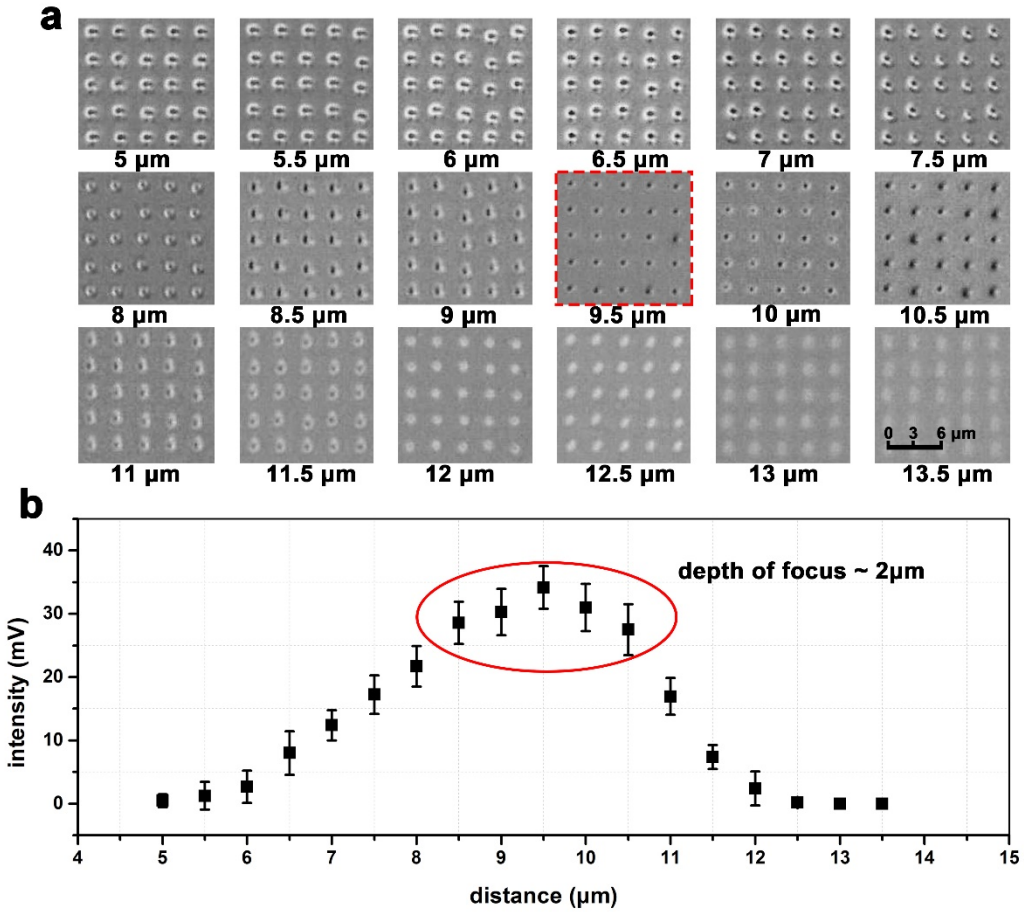

Supplementary Figure 10. The tolerance for the height fluctuation of the sample. **a,** Optical image of craters ablated by the output laser from microlensed fiber with different distances between fiber tip and sample surface on a smooth silica wafer. Each crater is made by a single laser pulse. The smallest size of sampling cater can be obtained at the focal length at 9.5 µm (with single-mode fiber). **b,** The effect of focal distances on signal intensity of Si^+ at *m/z* 28. Signal intensity reaches its highest value at the focal point. There are few changes in crater size or signal intensity in the plus or minus one-micron range of the focal point (9.5 µm). This makes the microlensed fiber-based MSI technique suitable for biological samples with height fluctuations within two microns, such as tissue slices and adherent single cells. Error bars represent the standard deviation of the signal intensity of Si^+ at *m/z* 28 of different sampling craters shown in **(a)** (n=25).

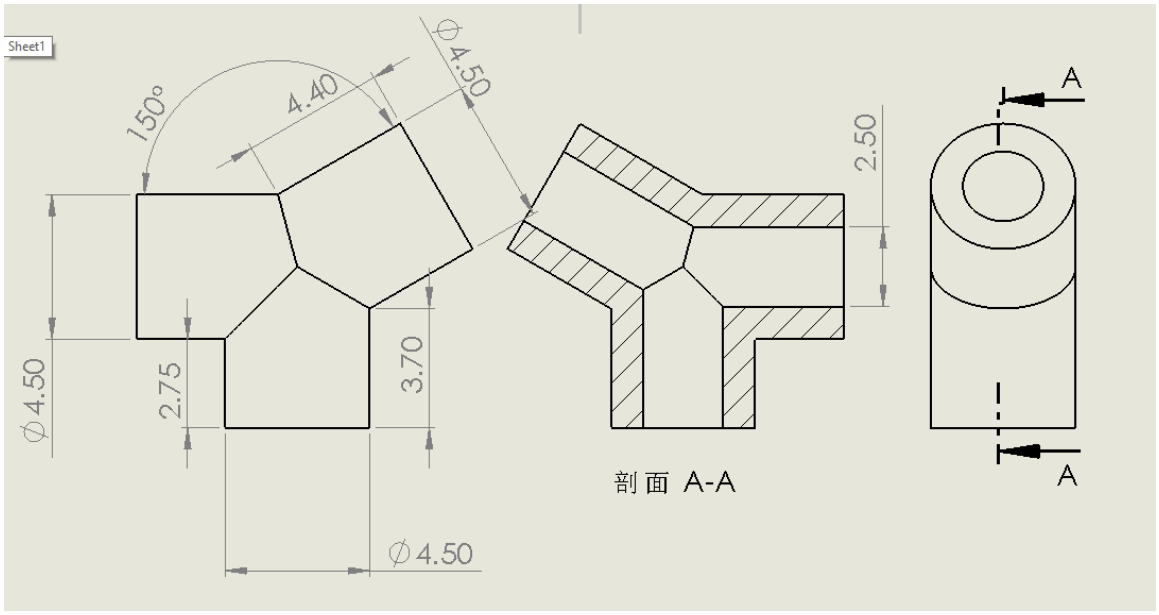

Supplementary Figure 11. Blueprint of the ablation chamber (shown in Supplementary Figure 4). (Left) Front view of the chamber. (Middle) Section view of A-A profile. (Right) Left view of the chamber.

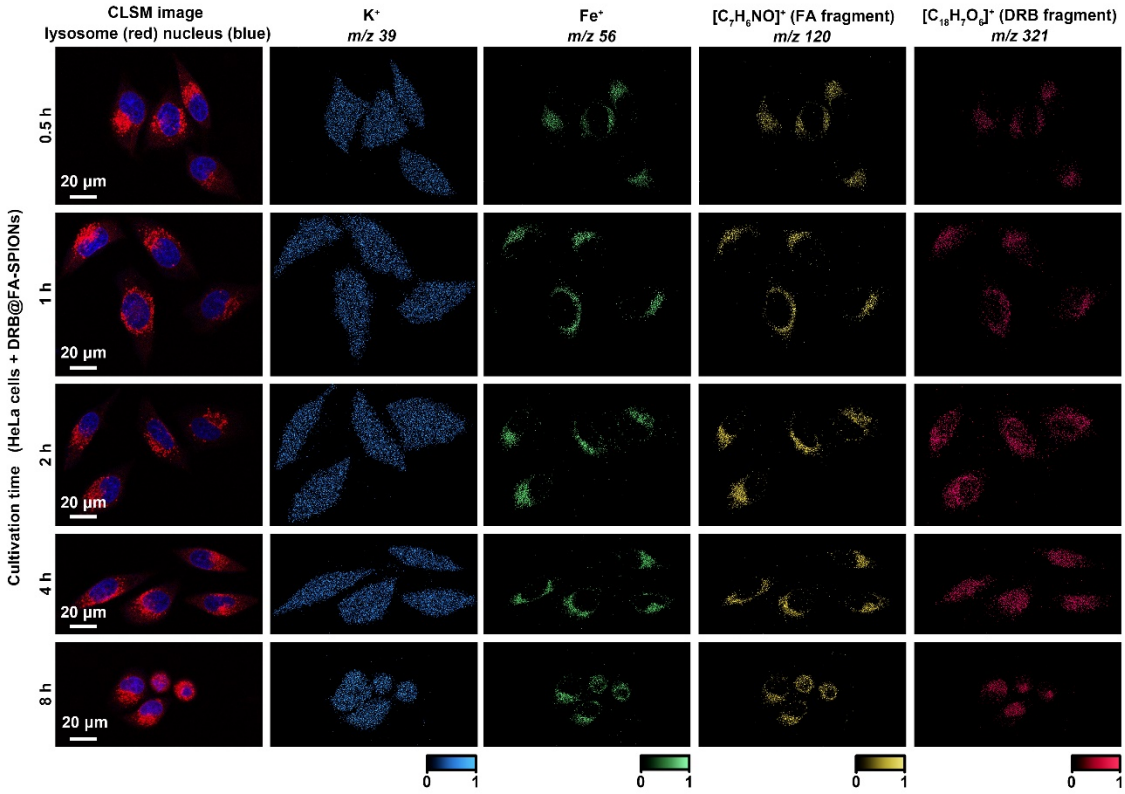

Supplementary Figure 12. Nanoscale MSI results of elements and drug molecules for the nanoparticle drug delivery system in HeLa cells at different cultivation times. Contrast of lysosomes and nucleus stained CLSM images and MS images of K^+, Fe^+, FA fragment $[C_7H_6NO]^+$ and DRB fragment $[C_{18}H_7O_6]^+$.